

Lawrence Berkeley National Laboratory

Recent Work

Title

Transverse momentum dependent parton distributions at small-x

Permalink

<https://escholarship.org/uc/item/7vd4p96n>

Authors

Xiao, BW
Yuan, F
Zhou, J

Publication Date

2017-08-01

DOI

10.1016/j.nuclphysb.2017.05.012

Peer reviewed



Transverse momentum dependent parton distributions at small- x

Bo-Wen Xiao ^a, Feng Yuan ^{b,*}, Jian Zhou ^c

^a Key Laboratory of Quark and Lepton Physics (MOE) and Institute of Particle Physics, Central China Normal University, Wuhan 430079, China

^b Nuclear Science Division, Lawrence Berkeley National Laboratory, Berkeley, CA 94720, USA

^c Key Laboratory of Particle Physics and Particle Irradiation (MOE) and School of Physics, Shandong University, Jinan 250100, China

Received 21 March 2017; received in revised form 8 May 2017; accepted 16 May 2017

Available online 23 May 2017

Editor: Hong-Jian He

Abstract

We study the transverse momentum dependent (TMD) parton distributions at small- x in a consistent framework that takes into account the TMD evolution and small- x evolution simultaneously. The small- x evolution effects are included by computing the TMDs at appropriate scales in terms of the dipole scattering amplitudes, which obey the relevant Balitsky–Kovchegov equation. Meanwhile, the TMD evolution is obtained by resumming the Collins–Soper type large logarithms emerged from the calculations in small- x formalism into Sudakov factors.

© 2017 The Authors. Published by Elsevier B.V. This is an open access article under the CC BY license (<http://creativecommons.org/licenses/by/4.0/>). Funded by SCOAP³.

1. Introduction

Transverse momentum dependent (TMD) parton distributions are among the most important and interesting topics to be fully investigated at the current and future facilities, including JLab 12 GeV upgrade, RHIC, and the planned electron–ion collider (EIC), and have been subjects of intense studies from both theory and experiment sides in the last decade or so. Most recent devel-

* Corresponding author.

E-mail address: fyuan@lbl.gov (F. Yuan).

opments focus on the particular kinematics where common interests have attracted the attentions from both the hadron physics and heavy ion physics communities, i.e., the TMDs at small- x . From the theoretical point of view, it has been shown that the TMDs at small- x are unified with the un-integrated gluon distributions (UGDs), which are widely applied in heavy ion physics, in particular, as an important ingredient to describe the initial conditions for heavy ion collisions at high energies. In the last few years, there have been tremendous progresses in connecting TMDs and small- x saturation physics.

There are two different unintegrated gluon distributions [1–7]. The first gluon distribution, which is known as the Weizsäcker–Williams (WW) gluon distribution, is calculated from the correlator of two classical gluon fields of relativistic hadrons [1,2]. The WW gluon distribution can be defined following the conventional gluon distribution [3,4]

$$xG^{(1)}(x, k_{\perp}) = \int \frac{d\xi^{-} d^2\xi_{\perp}}{(2\pi)^3 P^{+}} e^{ixP^{+}\xi^{-} - ik_{\perp} \cdot \xi_{\perp}} \langle P | F^{+i}(\xi^{-}, \xi_{\perp}) \mathcal{L}_{\xi}^{\dagger} \mathcal{L}_0 F^{+i}(0) | P \rangle, \quad (1)$$

where $F^{\mu\nu}$ is the gauge field strength tensor $F_a^{\mu\nu}$ and $\mathcal{L}_{\xi} = \mathcal{P} \exp\{-ig \int_{\xi}^{\infty} d\zeta^{-} A^{+}(\zeta, \xi_{\perp})\}$ is the gauge link in the adjoint representation. This gluon distribution can also be defined in the fundamental representation [6],

$$xG^{(1)}(x, k_{\perp}) = 2 \int \frac{d\xi^{-} d^2\xi_{\perp}}{(2\pi)^3 P^{+}} e^{ixP^{+}\xi^{-} - ik_{\perp} \cdot \xi_{\perp}} \langle P | \text{Tr} \left[F^{+i}(\xi^{-}, \xi_{\perp}) \mathcal{U}^{[+]\dagger} F^{+i}(0) \mathcal{U}^{[+]} \right] | P \rangle, \quad (2)$$

where the gauge link $\mathcal{U}_{\xi}^{[+]} = U^n [0, +\infty; 0] U^n [+\infty, \xi^{-}; \xi_{\perp}]$ with U^n being reduced to the light-like Wilson line in covariant gauge. Within the small- x color glass condensate (CGC) framework, this distribution can be written in terms of the correlator of four Wilson lines as [7,8],

$$xG^{(1)}(x, k_{\perp}) = -\frac{2}{\alpha_S} \int \frac{d^2x_{\perp}}{(2\pi)^2} \frac{d^2y_{\perp}}{(2\pi)^2} e^{-ik_{\perp} \cdot (x_{\perp} - y_{\perp})} \left\langle \text{Tr} [\partial_i U(x_{\perp})] U^{\dagger}(y_{\perp}) [\partial_i U(y_{\perp})] U^{\dagger}(x_{\perp}) \right\rangle_x, \quad (3)$$

where the Wilson line $U(x_{\perp})$ is defined as $U^n [-\infty, +\infty; x_{\perp}]$. The second gluon distribution, the Fourier transform of the dipole cross section, is defined in the fundamental representation

$$xG^{(2)}(x, k_{\perp}) = 2 \int \frac{d\xi^{-} d^2\xi_{\perp}}{(2\pi)^3 P^{+}} e^{ixP^{+}\xi^{-} - ik_{\perp} \cdot \xi_{\perp}} \langle P | \text{Tr} \left[F^{+i}(\xi^{-}, \xi_{\perp}) \mathcal{U}^{[-]\dagger} F^{+i}(0) \mathcal{U}^{[-]} \right] | P \rangle, \quad (4)$$

where the gauge link $\mathcal{U}_{\xi}^{[-]} = U^n [0, -\infty; 0] U^n [-\infty, \xi^{-}; \xi_{\perp}]$ stands for initial state interactions. Due to the gauge link in this gluon distribution being from $-\infty$ to $+\infty$, naturally this gluon distribution can be related to the color-dipole cross section evaluated from a dipole of size r_{\perp} scattering on the nucleus target [7,8],

$$xG^{(2)}(x, k_{\perp}) = \frac{q_{\perp}^2 N_c}{2\pi^2 \alpha_S} S_{\perp} \int \frac{d^2r_{\perp}}{(2\pi)^2} e^{-ik_{\perp} \cdot r_{\perp}} \frac{1}{N_c} \left\langle \text{Tr} U(0) U^{\dagger}(r_{\perp}) \right\rangle_x. \quad (5)$$

Similar analysis can also be extended to the polarization dependent cases [9–14]. Such identifications have laid solid foundation for the exploration of the nucleon/nuclei tomography in terms of parton distributions, which can be measured through various high energy hard scattering processes.

Meanwhile, the QCD evolution effects also play important roles in describing the scale dependence of these gluon distributions. This includes the small- x evolution, i.e., the BFKL/BK evolution [15,16], and the so-called TMD evolution, i.e., the Collins–Soper evolution [17,3]. With the small- x approximations applied in Eq. (3), (5), the small- x evolution effects are taken into account with the associated evolution equations. However, from those equations, the Collins–Soper evolution effects are not explicit. A recent quark target model calculation has shown that it is possible to treat the small x evolution and the TMD evolution in a unified and consistent way by directly computing the matrix element given in Eqs. (1), (4) in the small x limit [18]. The goal of this paper is to investigate the evolution effects for these TMDs, by taking into account both small- x and TMD evolution equations from the perspective of the TMD framework in terms of gauge links. Similar studies have been performed by Balitsky and Tarasov in Refs. [19] and Marzani in Ref. [20].

We follow closely the derivations in the previous publications [21,22], where it has been shown the above two resummations (Sudakov and small- x) can be performed consistently at the cross section level. To study the scale dependence of TMDs at small x , we go back to the full QCD definitions of the TMDs, in which the scale dependence naturally show up in the associated TMD factorization for hard scattering processes. In the gauge invariant definitions of the gluon distributions as shown in Eqs. (1), (4), there are un-canceled light-cone singularities from high order gluon radiations. The regularization introduces the scheme dependence for the TMDs and the associated factorizations.¹ In our calculation presented in this paper, we follow the Collins 2011 scheme [26], where the soft factor subtraction in the TMDs is applied to regulate the light-cone singularity. Similar to the case of the hard scattering processes studied in Refs. [21,22], the most important high order gluon radiation come from two regions: (1) soft gluon and (2) collinear gluon. The soft gluon radiation leads to the Collins–Soper evolution, whereas the collinear gluon contributes to the DGLAP resummation formulated in terms of the integrated parton distributions in the CSS resummation formalism. In our case, these collinear gluon radiation contributions actually become the small- x evolution contributions, which are described by the associated BK/JIMWLK equations [15,16,27,28]. The above two contributions are well separated in phase space. That is the reason that we can achieve resummations of large logarithms from these two sources consistently. The final results for the TMDs can be written as

$$xG^{(1)}(x, k_{\perp}, \zeta_c = \mu_F = Q) = -\frac{2}{\alpha_S} \int \frac{d^2x_{\perp} d^2y_{\perp}}{(2\pi)^4} e^{ik_{\perp} \cdot r_{\perp}} \mathcal{H}^{WW}(\alpha_S(Q)) e^{-S_{sud}(Q^2, r_{\perp}^2)} \times \mathcal{F}_{Y=\ln 1/x}^{WW}(x_{\perp}, y_{\perp}), \quad (6)$$

where $r_{\perp} = x_{\perp} - y_{\perp}$, ζ_c is the regulator for the end-point singularity in the TMD distributions in the Collins 2011 scheme, μ_F is the associated factorization scale. In the final factorization formula, these two scales are usually taken as the same as the hard momentum scale Q in hard scattering processes. Meanwhile, \mathcal{F}_Y^{WW} is the Fourier transform of the WW gluon distribution as in Eq. (3),

$$\mathcal{F}_Y^{WW}(x_{\perp}, y_{\perp}) = \left\langle \text{Tr} \left[\partial_{\perp}^{\beta} U(x_{\perp}) U^{\dagger}(y_{\perp}) \partial_{\perp}^{\beta} U(y_{\perp}) U^{\dagger}(x_{\perp}) \right] \right\rangle_Y \quad (7)$$

¹ After solving the evolution equations, the equivalence between different schemes can be proved order by order in perturbation theory [23–25].

and Y represents the rapidity of the gluon from the nucleus $Y \sim \ln(1/x)$. The Sudakov form factor contains all order resummation

$$\mathcal{S}_{sud} = \int_{c_0^2/r_\perp^2}^{Q^2} \frac{d\mu^2}{\mu^2} \left[A \ln \frac{Q^2}{\mu^2} + B \right], \quad (8)$$

where $c_0 = 2e^{-\gamma_E}$ with γ_E the Euler constant. The hard coefficients A and B can be calculated perturbatively: $A = \sum_{i=1}^{\infty} A^{(i)} \left(\frac{\alpha_s}{\pi}\right)^i$ and $B = \sum_{i=1}^{\infty} B^{(i)} \left(\frac{\alpha_s}{\pi}\right)^i$. Similarly, we can write down the result for the dipole-gluon TMD,

$$xG^{(2)}(x, k_\perp, \zeta_c = \mu_F = Q) = -\frac{2}{\alpha_s} \int \frac{d^2x_\perp d^2y_\perp}{(2\pi)^4} e^{ik_\perp \cdot r_\perp} \mathcal{H}^{DP}(\alpha_s(Q)) e^{-\mathcal{S}_{sud}(Q^2, r_\perp^2)} \times \nabla_{r_\perp}^{-2} \mathcal{F}_{Y=\ln 1/x}^{DP}(x_\perp, y_\perp), \quad (9)$$

where $\mathcal{F}_Y^{DP}(x_\perp, y_\perp)$ with $r_\perp \equiv x_\perp - y_\perp$ is defined as,

$$\mathcal{F}_Y^{DP}(x_\perp, y_\perp) = \left\langle \text{Tr} \left[U(x_\perp) U^\dagger(y_\perp) \right] \right\rangle_Y. \quad (10)$$

In the above equations, both \mathcal{F}_Y^{WW} and \mathcal{F}_Y^{DP} are the renormalized quadrupole and dipole amplitudes, respectively, which obey the associated small- x evolution equations. The TMD evolution effects are included in the Sudakov factor. The remaining factors, $\mathcal{H}^{WW}(\alpha_s(Q))$ and $\mathcal{H}^{DP}(\alpha_s(Q))$, which are of order 1, are the perturbative calculable finite hard parts.

We would like to emphasize that our approach is different from the previous works [18–22]. As mentioned above, the basic idea is the same as that in Refs. [21,22]. However, in this paper, we study the transverse momentum dependent parton distributions, which can be applied to various hard scattering processes. In Refs. [21,22], one particular hard process is studied. On the technique side, the TMDs contain the light-cone singularity, for which we will adopt Collins-11 (JCC) scheme to regulate such singularity and perform the associated resummation by solving the evolution equations. We note that in Ref. [18], the Ji-Ma-Yuan scheme has been applied.

Our approach is also different from those in Refs. [19,20]. In particular, the authors of Ref. [19] tried to derive a universal evolution equation for both large- x and small- x . In our study below, we focus only the small- x region, and we derive both Collins–Soper evolution and small- x BK-type evolution. These two are separate evolution equations, which is different from that in Refs. [19]. The paper of Ref. [20] studies the combined TMD and small- x resummations in the collinear factorization framework. In our paper, we study the parton distribution in dense medium of large nucleus, where the non-linear effects in the small- x evolution plays an important role. The latter is absent in the analysis of Ref. [20].

The rest of this paper is organized as follows. In Sec. 2, we present a brief review on the TMD evolution, i.e., the Collins–Soper evolution, and the CSS resummation [29] in the collinear framework. Here, the integrated parton distributions will be important non-perturbative inputs for the TMDs. They obey the DGLAP evolution equations. In Sec. 3, we compute the TMDs defined in Eqs. (1), (4) using the CGC approach and present our solutions for the TMDs with both Collins–Soper and small- x evolution effects. Finally, we conclude in Sec. 4.

2. TMDs in the collinear approach and the Collins–Soper evolution

Before presenting the calculations of TMDs in the CGC approach, it would be instructive to first briefly review how the Sudakov resummation is formulated in the collinear approach. We start with the TMD quark distribution. The un-subtracted TMD quark distribution is defined as

$$f_q^{unsub.}(x, k_\perp) = \frac{1}{2} \int \frac{d\xi^- d^2\xi_\perp}{(2\pi)^3} e^{-ix\xi^- P^+ + i\vec{\xi}_\perp \cdot \vec{k}_\perp} \left\langle PS \left| \bar{\psi}(\xi) \mathcal{L}_n^\dagger(\xi) \gamma^+ \mathcal{L}_n(0) \psi(0) \right| PS \right\rangle, \quad (11)$$

with the gauge link defined as $\mathcal{L}_n(\xi) \equiv \exp\left(-ig \int_0^\infty d\lambda v \cdot A(\lambda n + \xi)\right)$. As mentioned in the Introduction, there exist the light-cone singularities in the un-subtracted TMD distributions. In the Collins 2011 prescription, these singularities are canceled out by the soft factor,

$$\tilde{f}_q^{(sub.)}(x, r_\perp, \mu_F, \zeta_c) = f_q^{unsub.}(x, r_\perp) \sqrt{\frac{S^{\bar{n},v}(r_\perp)}{S^{n,\bar{n}}(r_\perp) S^{n,v}(r_\perp)}}, \quad (12)$$

with S^{v_1, v_2} defined as

$$S^{v_1, v_2}(r_\perp) = \langle 0 | \mathcal{L}_{v_2}^\dagger(r_\perp) \mathcal{L}_{v_1}^\dagger(r_\perp) \mathcal{L}_{v_1}(0) \mathcal{L}_{v_2}(0) | 0 \rangle. \quad (13)$$

Here, r_\perp is the Fourier conjugate variable with respect to the transverse momentum k_\perp , μ_F is the factorization scale. And ζ_c^2 is defined as $\zeta_c^2 = x^2(2v \cdot P)^2/v^2 = 2(xP^+)^2 e^{-2y_n}$ with y_n being the rapidity cut-off in the Collins-11 scheme. The second factor represents the soft factor subtraction with n and \bar{n} as the light-front vectors $n = (1^-, 0^+, 0_\perp)$, $\bar{n} = (0^-, 1^+, 0_\perp)$, whereas v is an off-light-front $v = (v^-, v^+, 0_\perp)$ with $v^- \gg v^+$.

2.1. Soft gluon radiation and the Collins–Soper evolution

At leading order, the quark TMD in the collinear factorization can be expressed as,

$$f_q(x, k_\perp)|^{(0)} = \delta^{(2)}(k_\perp) q(x), \quad (14)$$

where $q(x)$ represents the integrated quark distribution. In the Fourier transformation r_\perp space, we have

$$\tilde{f}_q(x, r_\perp)|^{(0)} = q(x). \quad (15)$$

At one-loop order, the most important contribution comes from soft gluon radiation, which leads to the Collins–Soper evolution equation for the TMDs. To illustrate the energy dependence, it is convenient to show the one-loop result,

$$f_q(x, k_\perp)|_{soft-real}^{(1)} = \frac{\alpha_s}{2\pi^2} \frac{1}{k_\perp^2} C_F \int \frac{dx'}{x'} q(x') \left\{ \delta(1 - \xi) \left(\ln \frac{\zeta_c^2}{k_\perp^2} \right) \right\}, \quad (16)$$

where $\xi = x/x'$ and ζ_c is defined above. The virtual diagram only contributes to the counter terms,

$$\tilde{f}_q(x, r_\perp)|_{vir}^{(1)} = \int \frac{dx'}{x'} q(x') \frac{\alpha_s}{2\pi} C_F \delta(1 - \xi) \left[-\frac{1}{\epsilon^2} - \frac{3}{2\epsilon} + \frac{1}{\epsilon} \ln \frac{\zeta_c^2}{\mu^2} \right], \quad (17)$$

where we have applied the dimensional regulation $d = 4 - 2\epsilon$. The virtual and soft contributions together give

$$\tilde{f}_q(x, r_\perp)|_{soft}^{(1)} = q(x) \frac{\alpha_s}{2\pi} C_F \left[\frac{1}{2} \left(\ln \frac{\zeta_c^2}{\mu^2} \right)^2 - \frac{1}{2} \left(\ln \frac{\zeta_c^2 r_\perp^2}{c_0^2} \right)^2 - \frac{3}{2\epsilon} \right], \quad (18)$$

with $c_0 = 2e^{-\gamma_E}$. Clearly, the above result demonstrates that we do have energy dependence.

2.2. Collinear gluon radiation and the DGLAP evolution

In addition, there are also collinear gluon radiation contributions, which can be resummed to all order in the CSS formalism as well. At one-loop order the collinear gluon takes the following expression,

$$f_q(x, k_\perp)|_{coll-real}^{(1)} = \frac{\alpha_s}{2\pi^2} \frac{1}{k_\perp^2} C_F \int \frac{dx'}{x'} q(x') \left\{ \frac{1 + \xi^2}{(1 - \xi)_+} + \frac{D - 2}{2} (1 - \xi) \right\}, \quad (19)$$

where D represents the number of transverse dimensions which implies $D = 2 - 2\epsilon$ in the dimensional regulation used in our calculations. In r_\perp space, it reads,

$$\begin{aligned} \tilde{f}_q(x, r_\perp)|_{coll}^{(1)} &= \frac{\alpha_s}{2\pi} C_F \int \frac{dx'}{x'} q(x') \left\{ \left(-\frac{1}{\epsilon} + \ln \frac{c_0^2}{r_\perp^2 \mu^2} \right) \mathcal{P}_{qq}(\xi) \right. \\ &\quad \left. + (1 - \xi) + \delta(1 - \xi) \left[\frac{3}{2} \ln \frac{r_\perp^2 \mu^2}{c_0^2} + \frac{3}{2\epsilon} \right] \right\}, \end{aligned} \quad (20)$$

where $\mathcal{P}_{qq}(\xi) = \left(\frac{1 + \xi^2}{1 - \xi} \right)_+$. At small- x , there is also important contribution from gluon splitting, which can be written as

$$f_q(x, k_\perp)|_{coll-real}^{(1)} = \frac{\alpha_s}{2\pi^2} \frac{1}{k_\perp^2} T_R \int \frac{dx'}{x'} g(x') \left\{ [\xi^2 + (1 - \xi)^2] + (D - 2)2\xi(1 - \xi) \right\}, \quad (21)$$

which contributes to both the integrated quark distribution and the TMD quark distribution in r_\perp -space.

Two evolution equations are derived for the TMDs: one is the energy evolution equation respect to ζ , the so-called Collins–Soper evolution equation [17]; one is the renormalization group equation associated with the factorization scale μ . After solving the evolution equations and expressing the TMDs in terms of the integrated parton distributions to have a complete resummation results, we can write,

$$\begin{aligned} \tilde{f}_q^{(sub.)}(x, r_\perp, \zeta_c = \mu_F = Q) &= e^{-S_{pert}^q(Q, r_\perp)} \tilde{\mathcal{F}}_q(\alpha_s(Q)) \\ &\quad \times \sum_i C_{q/i}(\mu_r/\mu) \otimes f_i(x, \mu), \end{aligned} \quad (22)$$

where $f_i(x, \mu)$ represent the relevant integrated parton distributions, and $\mu_r = c_0/r_\perp$. We have chosen the energy parameter $\zeta_c^2 = Q^2$ and the factorization scale $\mu_F = Q$ to resum large logarithms. The Sudakov factor can be written as

$$S_{pert}^q(Q, r_\perp) = \int_{\mu_r^2}^{Q^2} \frac{d\mu^2}{\mu^2} \left[A_q \ln \frac{Q^2}{\mu^2} + B_q \right], \quad (23)$$

where A and B are perturbative calculable: $A_q = \sum_{i=1} A_q^{(i)} (\alpha_s/\pi)^i$ and $B_q = \sum_{i=1} B_q^{(i)} (\alpha_s/\pi)^i$, with $A_q^{(1)} = \frac{1}{2} C_F$ and $B_q^{(1)} = -\frac{3}{4} C_F$. By choosing the scale $\mu = \mu_r$ for the integrated parton distribution in Eq. (22), the C -coefficients are defined as

$$C_{q/q'}(x, \mu = \mu_r) = \delta_{qq'} \left[\delta(1-x) + \frac{\alpha_s}{2\pi} C_F (1-x) \right], \quad (24)$$

for the quark–quark splitting case. In the Collins-11 (JCC) scheme [26], the scheme dependent term $\tilde{\mathcal{F}}$ takes a very simple form at one-loop order,

$$\tilde{\mathcal{F}}_q(\alpha_s(Q)) = 1 + \mathcal{O}(\alpha_s^2), \quad (25)$$

where α_s correction vanishes.

At small- x , the dominant contribution comes from the gluon splitting. This is represented by the collinear quark distribution dependence in Eq. (22), where $f_q(x, \mu_r)$ is driven by the gluon distribution at small- x in the collinear framework. Therefore, at small- x , we can find out that the TMD quark distribution behaves as $\sim g(x, \mu_r) \alpha_s \ln(\mu_r)$. This is also true in the CGC formalism, which will be discussed in Sec. 3.

2.3. TMD gluon distributions

Now let us also summarize some known results for the gluon TMD computed in the collinear framework. Again, we follow the Collins 2011 scheme to define the TMD gluon distributions. The un-subtracted gluon TMD is defined as

$$x f_g^{unsub.}(x, k_\perp) = \int \frac{d\xi^- d^2 \xi_\perp}{P^+ (2\pi)^3} e^{-ixP^+ \xi^- + i\vec{k}_\perp \cdot \vec{\xi}_\perp} \times \left\langle P | F_{a\mu}^+(\xi^-, \xi_\perp) \mathcal{L}_{nab}^\dagger(\xi^-, \xi_\perp) \mathcal{L}_{nbc}(0, 0_\perp) F_c^{\mu+}(0) | P \right\rangle, \quad (26)$$

where the associated gauge link is in adjoint representation. In the Collins 2011 scheme, we define

$$x f_g^{(sub)}(x, r_\perp, \mu, \zeta_c) = x f_g^{unsub.}(x, r_\perp) \sqrt{\frac{S^{\bar{n}, v}(r_\perp)}{S^{n, \bar{n}}(r_\perp) S^{n, v}(r_\perp)}}, \quad (27)$$

where S^{v_1, v_2} are defined similarly as those in the quark distribution but in the adjoint representations. In the collinear approach where f_g denotes the above defined gluon distribution, it is straightforward to calculate the real correction contribution,

$$f_g^{(sub)}(x, k_\perp)|_{real}^{(1)} = \frac{\alpha_s}{\pi^2} \frac{1}{k_\perp^2} C_A \int \frac{dx'}{x'} g(x') \left\{ \frac{\xi}{(1-\xi)_+} + \frac{1-\xi}{\xi} + \xi(1-\xi) + \delta(1-\xi) \left(\ln \frac{\zeta_c^2}{k_\perp^2} \right) \right\}. \quad (28)$$

In r_\perp space, one has,

$$\begin{aligned} \tilde{f}_g^{(sub)}(x, r_\perp)|_{real}^{(1)} &= \frac{\alpha_s}{2\pi} C_A \int \frac{dx'}{x'} g(x') \left\{ \left(-\frac{1}{\epsilon} + \ln \frac{c_0^2}{r_\perp^2 \mu^2} \right) [\mathcal{P}_{gg}(\xi) - 2\beta_0 \delta(1-\xi)] \right\} \\ &+ g(x) \frac{\alpha_s}{2\pi} C_A \left\{ \frac{1}{\epsilon^2} - \frac{1}{\epsilon} \ln \frac{\zeta_c^2}{\mu^2} + \frac{1}{2} \left(\ln \frac{\zeta_c^2}{\mu^2} \right)^2 - \frac{1}{2} \left(\ln \frac{\zeta_c^2 r_\perp^2}{c_0^2} \right)^2 \right\}, \end{aligned} \quad (29)$$

where $\mathcal{P}_{gg}(\xi) = \frac{2(1-\xi)}{\xi} + \frac{2\xi}{(1-\xi)_+} + 2\xi(1-\xi) - 2\beta_0\delta(1-\xi)$ and $\beta_0 = (11 - 2N_f/3)/12$. After removing the UV divergence, the virtual contribution is given by,

$$\tilde{f}_g^{(sub)}(x, r_\perp)|_{vir}^{(1)} = g(x) \frac{\alpha_s}{2\pi} C_A \left[-\frac{1}{\epsilon^2} - 2\beta_0 \frac{1}{\epsilon} + \frac{1}{\epsilon} \ln \frac{\zeta_c^2}{\mu^2} \right]. \quad (30)$$

Combining the real contribution and the virtual contribution, we end up with,

$$\begin{aligned} \tilde{f}_g^{(sub)}(x, r_\perp)^{(1)} &= \frac{\alpha_s}{2\pi} C_A \int \frac{dx'}{x'} g(x') \left\{ \left(-\frac{1}{\epsilon} + \ln \frac{c_0^2}{r_\perp^2 \mu^2} \right) \mathcal{P}_{gg}(\xi) \right\} \\ &+ g(x) \frac{\alpha_s}{2\pi} C_A \left\{ \frac{1}{2} \left(\ln \frac{\zeta_c^2}{\mu^2} \right)^2 - \frac{1}{2} \left(\ln \frac{\zeta_c^2 r_\perp^2}{c_0^2} \right)^2 + 2\beta_0 \ln \frac{r_\perp^2 \mu^2}{c_0^2} \right\}, \quad (31) \end{aligned}$$

where the double and single IR poles are canceled out. The remaining collinear divergence can be removed by introducing a renormalized integrated gluon distribution. Following the same procedure as for the quark TMD case, all large logarithms appear in the above formula can be summed into the Sudakov factor. All order resummation result can be written, similarly,

$$\begin{aligned} \tilde{f}_g^{(sub.)}(x, r_\perp, \zeta_c = \mu_F = Q) &= e^{-S_{pert}^g(Q, r_\perp)} \tilde{\mathcal{F}}_g(\alpha_s(Q)) \\ &\times \sum_i C_{g/i}(\mu_r/\mu) \otimes f_i(x, \mu), \quad (32) \end{aligned}$$

where the Sudakov factor takes the same form as in Eq. (23),

$$S_{pert}^g(Q, r) = \int_{\mu_f^2}^{Q^2} \frac{d\mu^2}{\mu^2} \left[A_g \ln \frac{Q^2}{\mu^2} + B_g \right], \quad (33)$$

with $A_g^{(1)} = \frac{1}{2}C_A$ and $B_g^{(1)} = -\beta_0 C_A$. Both $C_{g/g}$ and $\tilde{\mathcal{F}}_g$ with $\mu = \mu_r$ in Eq. (32) vanishes at one-loop order.

At small x , we can further simplify the above expression by approximating $\mathcal{P}_{gg} \approx \frac{2}{\xi}$ and treating $x'_g g(x'_g)$ as a slowly varying function of x' . One then can trivially carry out x' integration,

$$\begin{aligned} x \tilde{f}_g^{(sub)}(x, r_\perp)^{(1)} &= \frac{\alpha_s C_A}{\pi} x g(x) \ln \frac{1}{x} \left(-\frac{1}{\epsilon} + \ln \frac{c_0^2}{r_\perp^2 \mu^2} \right) \\ &+ x g(x) \frac{\alpha_s}{2\pi} C_A \left\{ \frac{1}{2} \left(\ln \frac{\zeta_c^2}{\mu^2} \right)^2 - \frac{1}{2} \left(\ln \frac{\zeta_c^2 r_\perp^2}{c_0^2} \right)^2 + 2\beta_0 \ln \frac{r_\perp^2 \mu^2}{c_0^2} \right\}, \quad (34) \end{aligned}$$

where the large logarithm $\ln \frac{1}{x}$ should also be properly resummed to improve perturbative calculation. We will address this issue in the next section.

3. TMDs in the CGC approach and the Collins–Soper evolution

It has been argued that at sufficient small x the logarithm $\ln \frac{1}{x}$ is more important than the collinear logarithm $\ln \frac{Q^2}{\mu^2}$. The leading region, which gives rise to $\ln \frac{1}{x}$ enhancement, is the so-called strong rapidity ordering region rather than the strong k_T ordering region, i.e. the leading

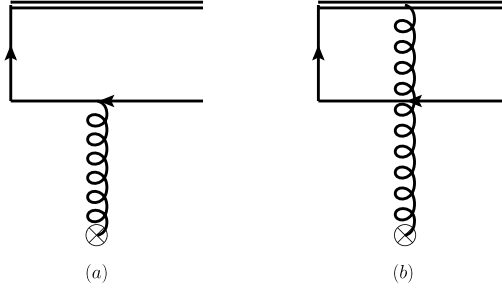


Fig. 1. The transverse momentum dependent quark distribution calculated in the small- x formalism for the Drell–Yan process, where the double line represents the gauge link contributions from the gauge invariant definition of the quark distribution for this process.

region in the collinear approach. As a consequence, one should keep incoming parton transverse momentum when computing physical observables or parton TMDs. Note that the Collins–Soper type logarithms can be equally important as the logarithm $\ln \frac{1}{x}$ depending on kinematics in a physical process. We are aiming to resum these two type large logarithms simultaneously in a unified and consistent framework. To this end, we formulate the calculation of parton TMDs in the CGC framework. We start with discussing the small x quark TMDs.

3.1. TMD quark at small- x

The quark distribution has been evaluated in the small- x formalism in the literature [30–32]. It is interesting to note that the TMD quark distribution for the DIS and Drell–Yan processes are the same, which reflects the universality of the quark distribution. In this subsection, we review these results, in the context of the TMD definitions with associated gauge links.

For the Drell–Yan process, the gauge invariant quark distribution contains the gauge link in the fundamental representation pointing to the direction towards $-\infty$, whereas that for the DIS process the gauge link goes to $+\infty$. Because of this difference, there are different diagrams that contribute to the TMD quark distributions for these two processes. We will show that they are the same in the final result despite the fact that they take the very different forms initially.

The TMD quark in Drell–Yan process can be calculated from the diagrams in Fig. 1, with the following contributions,

$$xq^{(DY)}(x, k_{\perp}) = \frac{N_c}{8\pi^4} \int d\xi \int d^2k_{g\perp} F_{x_g}(k_{g\perp}) A(k_{g\perp}, k_{\perp}), \quad (35)$$

where $\xi = x/x_g$ with x_g standing for the momentum fraction of the incoming gluon, and $F(q_{\perp})$ is the well-known dipole gluon distribution,

$$F_{x_g}(k_{g\perp}) \equiv \int \frac{d^2x_{\perp} d^2y_{\perp}}{(2\pi)^2} e^{-ik_{g\perp} \cdot (x_{\perp} - y_{\perp})} \frac{1}{N_c} \langle U(x_{\perp}) U^{\dagger}(y_{\perp}) \rangle_{x_g}. \quad (36)$$

The coefficient A is defined as

$$A(k_{g\perp}, k_{\perp}) = \left[\frac{\vec{k}_{\perp} |k_{\perp} - k_{g\perp}|}{(1 - \xi)k_{\perp}^2 + \xi(k_{\perp} - k_{g\perp})^2} - \frac{\vec{k}_{\perp} - \vec{k}_{g\perp}}{|k_{\perp} - k_{g\perp}|} \right]^2. \quad (37)$$

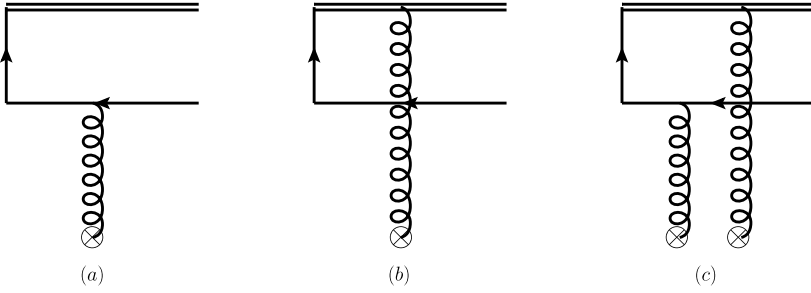


Fig. 2. Same as Fig. 1, but for the DIS process, where the gauge link goes to $+\infty$.

In the above equation, there is no divergence of the integral over ξ , and in the leading logarithmic small- x approximation, we can integrate out ξ and obtain the following expression,

$$xq^{(DY)}(x, k_{\perp}) = \frac{N_c}{4\pi^4} \int d^2k_{g\perp} F_x(k_{g\perp}) \left(1 - \frac{k_{\perp} \cdot (k_{\perp} - k_{g\perp})}{k_{\perp}^2 - (k_{\perp} - k_{g\perp})^2} \ln \frac{k_{\perp}^2}{(k_{\perp} - k_{g\perp})^2} \right). \quad (38)$$

However, for the DIS process, because the gauge link goes to $+\infty$, there is an additional diagram contributing to the TMD quark distribution, as shown in Fig. 2(c). In particular, this diagram contains the following integral in the momentum space,

$$\begin{aligned} \text{Fig. 2(c)}|_{\text{DIS}} &\propto \int \frac{dk_{g1}^+}{2\pi} \left(\frac{1}{-k_{g1}^+ + i\epsilon} \right) \\ &\times \left(\frac{1}{2(k_{g1}^+ - k_g^+)k_1^- + (2k_{1\perp} - k_{g\perp} + k_{g1\perp}) \cdot (k_{g\perp} - k_{g1\perp}) + i\epsilon} \right), \end{aligned} \quad (39)$$

where k_{g1} represents the momentum connecting to the gauge link, k_1 for the final state antiquark momentum. The first factor comes from the gauge link propagator, whereas the second factor from the quark propagator. Clearly, there is a non-vanishing contribution in the above integral, because the two poles are at the opposite half planes in k_{g1}^+ integral. However, for DY case, because the gauge link goes to $-\infty$, the first factor would change the sign for $i\epsilon$, and this diagram leads to

$$\begin{aligned} \text{Fig. 2(c)}|_{\text{DY}} &\propto \int \frac{dk_{g1}^+}{2\pi} \left(\frac{1}{-k_{g1}^+ - i\epsilon} \right) \\ &\times \left(\frac{1}{2(k_{g1}^+ - k_g^+)k_1^- + (2k_{1\perp} - k_{g\perp} + k_{g1\perp}) \cdot (k_{g\perp} - k_{g1\perp}) + i\epsilon} \right). \end{aligned} \quad (40)$$

Clearly, it vanishes because the two poles are in the same half plane in k_{g1}^+ integral.

The rest of the calculations are straightforward, which gives the following expression for the quark distribution in DIS process,

$$\begin{aligned} xq^{(DIS)}(x, k_{\perp}) &= \frac{N_c}{8\pi^4} \int_0^1 d\xi \int d^2k_{g\perp} d^2k_{g1\perp} d^2k'_{g1\perp} \end{aligned}$$

$$\begin{aligned}
& \times \int \frac{d^2x_1 d^2x_2 d^2y_1 d^2y_2}{(2\pi)^6} e^{ik_{g1\perp} \cdot (x_1 - x_2)} e^{ik_{g\perp} \cdot (x_2 - y_2)} e^{-ik'_{g1\perp} \cdot (y_1 - y_2)} \\
& \times \frac{(k_{\perp} - k_{g1\perp}) \cdot (k_{\perp} - k'_{g1\perp})(k_{\perp} - k_{g\perp})^2}{\left[\xi(k_{\perp} - k_{g\perp})^2 + (1 - \xi)(k_{\perp} - k_{g1\perp})^2 \right] \left[\xi(k_{\perp} - k_{g\perp})^2 + (1 - \xi)(k_{\perp} - k'_{g1\perp})^2 \right]} \\
& \times \frac{1}{N_c} \left[\langle U(x_1)U^\dagger(x_2)U(y_2)U^\dagger(y_1) \rangle - \langle U(x_1)U^\dagger(x_2) \rangle - \langle U(y_2)U^\dagger(y_1) \rangle + 1 \right]. \quad (41)
\end{aligned}$$

It looks very different as compared to that for the Drell–Yan process. However, one can show that it is identical to the Drell–Yan quark TMD after a few steps of algebraic manipulations. We start with defining a new variable $\epsilon_f^2 = \xi(k_{\perp} - k_{g\perp})^2 / (1 - \xi)$ and changing integration variable $\xi \rightarrow \epsilon_f^2$. The integrand then no longer depends on $k_{g\perp}$. The $k_{g\perp}$ integration thus can be trivially carried out. As a result, the four point function in the last line collapses into the two point function after integrating over y_2 . One then arrives at

$$\begin{aligned}
& xq^{(DIS)}(x, k_{\perp}) \\
& = \frac{N_c}{8\pi^4} \int_0^\infty d\epsilon_f^2 \int d^2k_{g1\perp} d^2k'_{g1\perp} \int \frac{d^2x_1 d^2x_2 d^2y_1}{(2\pi)^4} e^{ik_{g1\perp} \cdot (x_1 - x_2)} \\
& \times e^{-ik'_{g1\perp} \cdot (y_1 - x_2)} \frac{(k_{\perp} - k_{g1\perp}) \cdot (k_{\perp} - k'_{g1\perp})}{\left[\epsilon_f^2 + (k_{\perp} - k_{g1\perp})^2 \right] \left[\epsilon_f^2 + (k_{\perp} - k'_{g1\perp})^2 \right]} \\
& \times \frac{1}{N_c} \left\{ \langle U(x_1)U^\dagger(y_1) \rangle - \langle U(x_1)U^\dagger(x_2) \rangle - \langle U(x_2)U^\dagger(y_1) \rangle + 1 \right\}, \quad (42)
\end{aligned}$$

which can be straightforwardly casted into the following expression

$$\begin{aligned}
xq^{(DIS)}(x, k_{\perp}) & = \frac{N_c}{8\pi^4} \int_0^\infty d\epsilon_f^2 \int d^2k_{g\perp} \int \frac{d^2x_1 d^2y_1}{(2\pi)^2} e^{ik_{g\perp} \cdot (x_1 - y_1)} \\
& \times \left[\frac{\vec{k}_{\perp} - \vec{k}_{g\perp}}{\epsilon_f^2 + (k_{\perp} - k_{g\perp})^2} - \frac{\vec{k}_{\perp}}{\epsilon_f^2 + k_{\perp}^2} \right]^2 \frac{1}{N_c} \langle U(x_1)U^\dagger(y_1) \rangle, \quad (43)
\end{aligned}$$

with some integration variables renamed. It now becomes evident that the above result for the DIS quark TMD is the same as that in the Drell–Yan process after changing integration variable $\epsilon_f^2 \rightarrow \xi$ with $\epsilon_f^2 = \xi(k_{\perp} - k_{g\perp})^2 / (1 - \xi)$. As such, the universality between the DIS quark TMD and the Drell–Yan quark TMD is verified as expected.

The universality of the spin-averaged TMD quark distributions in the DIS and DY processes can be proven by applying the combined parity and time-reversal invariance of QCD. It is nice that our explicit calculations above have demonstrated this universality, although there are different diagrams for the two cases (as shown in Figs. 1 and 2 for the DY and DIS processes, respectively).

A number of interesting features of this quark distribution have been discussed in the literature [30,31]. For example, in the small k_{\perp} limit, the quark distribution saturates: $xq(x, k_{\perp})|_{k_{\perp} \rightarrow 0} \propto N_c / 4\pi^4$; in the large k_{\perp} limit, it has power-law behavior $xq(x, k_{\perp})|_{k_{\perp} \gg Q_s} \propto Q_s^2 / k_{\perp}^2$. Here Q_s^2 is the saturation momentum which is proportional to the target gluon density $xG(x)$. Because of these behaviors, it is legitimate to Fourier transform the above expression

into the r_\perp -space,

$$\tilde{f}_{qCGC}(x, r_\perp) = \int d^2k_\perp e^{ik_\perp \cdot r_\perp} q(x, k_\perp), \tag{44}$$

where $q(x, k_\perp)$ follows the result calculated in the CGC formalism as in Eq. (38).

Note that both the Collins–Soper type large logarithm and the small x logarithm $\ln \frac{1}{x}$ are absent at leading order. Beyond the leading order contributions, we anticipate that the higher order gluon radiation (for instance, a gluon radiated from the gauge link) will generate the Sudakov logarithms in the soft gluon limit, which can be resummed by solving the associated Collins–Soper evolution equation. Meanwhile, the next to leading order contribution from the so-called strong rapidity ordering region will give rise to the large logarithm $\ln \frac{1}{x}$ enhancement. Such contribution should be absorbed into the renormalized dipole amplitude whose rapidity dependence is governed by the BK equation. After removing two different type large logarithms by means of the Collins–Soper and the BK equations, respectively, we are left with finite NLO correction to the hard coefficient.

To implement both TMD and small- x evolution effects, we substitute $f_q(x, \mu = \mu_r)$ in Eq. (22) with the above calculation from the small- x physics,

$$f_q(x, \mu_r) \rightarrow \tilde{f}_{qCGC}(x, r_\perp). \tag{45}$$

One can justify the above identification (substitution) in the small- r_\perp limit, which corresponds to the large transverse momentum. This is because the integrated quark distribution at small- x is proportional to the integrated gluon distribution with logarithmic dependence on the scale $x f_q(x, \mu_r) \propto x g(x, \mu_r) \ln(\mu_r)$, which is consistent with the CGC calculation of $\tilde{f}_q(x, r_\perp) \propto Q_s^2 \ln(1/r_\perp)$.

In the end, we have the following formula for the TMD quark in the CGC formalism,

$$\tilde{f}_q(x, r_\perp, \zeta_c = \mu_F = Q) |_{CGC} = e^{-S_{pert}^q(Q, r_\perp)} \tilde{f}_{qCGC}(x, r_\perp), \tag{46}$$

where the Sudakov factor takes the same form as in the last section, Eq. (23). In practice, we should implement the non-perturbative part of the Sudakov factor [26] as well.

It is interesting to check the small- r_\perp , i.e., the $r_\perp \ll 1/Q_s$ behavior, in the above equation. We first notice that the Fourier transform in Eq. (44) is dominant by the large k_\perp behavior of $f_q(x, k_\perp)$ of Eq. (38), and then write

$$\tilde{f}_{qCGC}(x, r_\perp) |_{r_\perp \ll 1/Q_s} \propto \int_{Q_s}^{1/r_\perp} d^2k_\perp \frac{Q_s^2}{k_\perp^2} \sim x G(x, 1/r_\perp) \alpha_s \ln(Q_s r_\perp), \tag{47}$$

where we have applied the approximation that the saturation scale Q_s is proportional to the gluon distribution at small- x . We have also dropped the exponential factor to simplify the derivation. This is consistent with the power counting analysis in the last section where $\mu_r = c_0/r_\perp$.

3.2. TMD gluon at small- x

The TMD gluon distributions can be calculated similarly. The operator definitions given in the Introductions are the un-subtracted gluon TMDs. In the Collins 2011 scheme, we introduce the same subtraction method as the quark distribution used above

$$f_g^{(sub.)}(x, r_\perp, \mu_F, \zeta_c) = f_g^{unsub.}(x, r_\perp) \sqrt{\frac{S^{\bar{n}, v}(r_\perp)}{S^{n, \bar{n}}(r_\perp) S^{n, v}(r_\perp)}}, \tag{48}$$

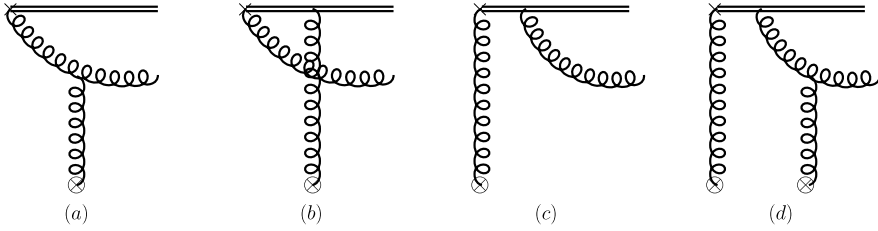


Fig. 3. The one-loop real gluon radiation contribution to the TMD gluon distribution with gauge link to $-\infty$ at small- x in the CGC framework. This gluon distribution can be used to describe the Higgs boson production in pA collisions. The crosses represent the probing gluon momentum (x, k_\perp) where x is the longitudinal momentum fraction and k_\perp is the transverse momentum.

with S^{v_1, v_2} defined in the adjoint representation and f_g representing either of $G^{(1)}$ and $G^{(2)}$ distributions. The soft gluon contributions are the same for both distributions. This implies that they obey the same Collins–Soper evolution equation.

We can calculate the above subtracted TMD gluon distributions in the CGC framework. At the leading order, they are reduced to the expressions presented in the Introduction, respectively (without evolution effects). At one-loop order, we again have soft and collinear gluon radiation contributions. The divergence in the soft gluon radiation is regulated by the soft factor subtraction, which is the same as the collinear approach. The remaining finite part contributes to the Delta function with large Sudakov logarithms. This part demonstrates that the TMD gluon distributions at small- x obey the same Collins–Soper evolution equation. To this end, we carry out calculations for the various TMD gluon distributions at small- x in the CGC framework at one-loop order as follows.

3.2.1. WW gluon distribution in Higgs boson production process

As a first example, we calculate the WW-gluon distribution in the Higgs boson production process, where the gauge link in the TMD definition goes to $-\infty$. At the leading order, the gluon distribution can be written as

$$xG_{(-\infty)}^{(WW)} = \frac{-2}{\alpha_s} \mathcal{F}^{(WW)}(x, k_\perp) = -\frac{2}{\alpha_s} \int \frac{d^2x_\perp d^2y_\perp}{(2\pi)^4} e^{ik_\perp \cdot (x_\perp - y_\perp)} \mathcal{F}^{WW}(x_\perp, y_\perp), \quad (49)$$

which is related to the quadruple correlation $\mathcal{F}^{WW}(x_\perp, y_\perp)$ defined in the Introduction in the CGC framework. At one-loop order, the Feynman diagrams of real gluon radiation are illustrated in Fig. 3 with the gauge link going to $-\infty$.

The diagrams in Fig. 3(a) and (b) depend on the same Wilson line, which is an adjoint representation Wilson line from $-\infty$ to $+\infty$. Therefore, we can combine these two diagrams together,

$$\begin{aligned} \text{Fig. 3(a, b)} &\propto \int \frac{d^2x_\perp}{(2\pi)^2} e^{ik_{g\perp} \cdot x_\perp} \frac{1}{T_F} \text{Tr} \left[T^b U(x_\perp) T^a U^\dagger(x_\perp) \right] \\ &\times \frac{1}{2} \left[(1 - \xi) \left(\frac{k_\perp^\alpha k_\perp^\nu}{(1 - \xi)k_\perp^2 + \xi k_{1\perp}^2} - \frac{k_{1\perp}^\alpha k_{1\perp}^\nu}{k_{1\perp}^2} \right) \right. \\ &\left. + \xi k_{1\perp}^2 \frac{g_\perp^{\alpha\nu}}{2} \left(\frac{1}{k_{1\perp}^2} - \frac{1}{(1 - \xi)k_\perp^2 + \xi k_{1\perp}^2} \right) \right], \quad (50) \end{aligned}$$

where $\xi = x/x_g$ is the same as used above, and $k_{g\perp} = k_{\perp} + k_{1\perp}$ with the radiated gluon transverse momentum being $k_{1\perp}$. Clearly, in the above result, there is no singularity at the end point of $\xi \rightarrow 1$. That means they do not contribute to the Sudakov logarithms. However, when $\xi \ll 1$, they play important role for the small- x evolution for the WW-gluon distribution.

The end point singularity actually comes from the diagrams in Fig. 3(c) and (d). Their contributions are proportional to the following expression,

$$\begin{aligned} \text{Fig. 3(c, d)} \propto & \int \frac{d^2 k_{g1\perp}}{(2\pi)^2} \frac{k_{\perp}^{\alpha} - k_{g1\perp}^{\alpha}}{(k_{\perp} - k_{g1\perp})^2} \int d^2 x_1 d^2 x_2 e^{ik_{g1\perp} \cdot (x_1 - x_2)} e^{ik_{g\perp} \cdot x_2} \\ & \times \text{Tr} \left[U^{\dagger}(x_2) T^b U(x_2) \left[i \partial_{\perp}^{\nu} U^{\dagger}(x_1) U(x_1), T^a \right] \right], \end{aligned} \quad (51)$$

which also contributes to the small- x evolution. To see this more clearly, we can compute the amplitude square of the above term, and find that it is proportional to

$$[\text{Fig. 3(c, d)}]^2 \propto \frac{1}{(k_{\perp} - k_{g\perp})^2} \frac{\alpha_s}{2\pi^2} C_A \int \frac{d\xi}{\xi(1-\xi)} \mathcal{F}^{(WW)}(x_g, k_{g\perp}). \quad (52)$$

The above expression contains two divergent contributions: one with $\xi = 1$ and the other with $\xi = 0$, which correspond to the end-point singularity and small- x divergence, respectively. The end-point singularity of $\xi = 1$ will be canceled by the soft factor subtraction following the Collins 2011 scheme. We would like to emphasize that the soft factor subtraction only applies to the contribution at the end point of $\xi = 1$. Meanwhile, the small- x divergence will be absorbed into the relevant small- x evolution for the WW-gluon distributions.

We can summarize the total contributions from Fig. 3 in the following expression,

$$\begin{aligned} \text{Fig. 3} \propto & \left[\frac{k_{1\perp}^{\alpha} k_{1\perp}^{\nu} - \epsilon_f^2 \frac{g_{1\perp}^{\alpha\nu}}{2}}{k_{1\perp}^2 + \epsilon_f^2} - \frac{k_{\perp}^{\alpha} k_{\perp}^{\nu} - \epsilon_f^2 \frac{g_{\perp}^{\alpha\nu}}{2}}{k_{\perp}^2 + \epsilon_f^2} \right] \Gamma_B(k_{g\perp}) \\ & + \int \frac{d^2 k_{g1\perp}}{(2\pi)^2} \frac{k'_{1\perp}{}^{\alpha}}{k'_{g1\perp}{}^2} \Gamma_A^{\nu}(k_{g1\perp}, k_{g2\perp}), \end{aligned} \quad (53)$$

where $k_{1\perp} = k_{\perp} - k_{g\perp}$, $k'_{1\perp} = k_{\perp} - k_{g1\perp}$, $\epsilon_f^2 = \xi k_{1\perp}^2 / (1 - \xi)$ and Γ_A and Γ_B are defined as

$$\begin{aligned} \Gamma_A^{\nu} &= \int d^2 x_{1\perp} d^2 x_{2\perp} e^{ik_{g1\perp} \cdot x_{1\perp} + ik_{g2\perp} \cdot x_{2\perp}} \text{Tr} \left[U^{\dagger}(x_2) T^b U(x_2) [i \partial_{\perp}^{\nu} U^{\dagger}(x_1) U(x_1), T^a] \right], \\ \Gamma_B &= \int d^2 x_{\perp} e^{ik_{g\perp} \cdot x_{\perp}} \frac{1}{T_F} \text{Tr} \left[T^b U(x_{\perp}) T^a U^{\dagger}(x_{\perp}) \right]. \end{aligned} \quad (54)$$

With the above notations, the end point singularity is represented by the limit $\epsilon_f^2 \rightarrow +\infty$, while the small- x singularity is obtained by taking $\epsilon_f^2 \rightarrow 0$. Because the end point singularity is canceled out by the soft factor subtraction, we do not need to consider a particular regulator or cutoff in the phase space integral. However, for the small- x part, we have to consider a proper regulator or we have to impose a kinematic constraint. In this case, because the lower limit for ξ is x of the probing gluon momentum fraction, the integral limit for ϵ_f^2 will be around $k_{1\perp}^2/x$. Therefore, the small- x singularity will be represented by $\ln(1/x)$ in the end. The phase space

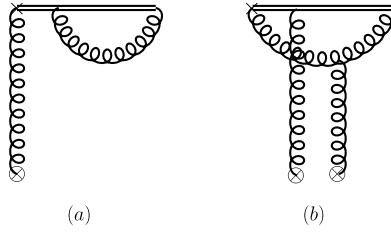


Fig. 4. The one-loop virtual gluon radiation contribution to the WW-type of TMD gluon distribution. The virtual diagrams are the same for the Drell–Yan type and DIS type of gluon distributions. Again, the crosses represent the probing gluon momentum (x, k_{\perp}) where x is the longitudinal momentum fraction and k_{\perp} is the transverse momentum.

integral is straightforward, and we obtain the real gluon radiation contribution at one-loop order,

$$xG_{(-\infty)}^{(WW)}|_{real} = \frac{\alpha_s}{2\pi^2} C_A \left\{ \int d^2k_{g\perp} \left(\frac{-2}{\alpha_s} \right) \mathcal{F}^{(WW)}(x, k_{g\perp}) \frac{1}{(k_{\perp} - k_{g\perp})^2} \ln \frac{\zeta_c^2}{(k_{\perp} - k_{g\perp})^2} + \ln \left(\frac{1}{x} \right) \left(\frac{-2}{\alpha_s} \right) \int \mathbf{K}_{\text{DMMX}(r)} \otimes \mathcal{F}^{(WW)}(x_g, k_{\perp}) \right\}, \quad (55)$$

where ζ_c is the regulating parameter in the Collins 2011 scheme and has been defined in Sec. 2, and $\mathbf{K}_{\text{DMMX}(r)}$ represents the real part of the BK-type of the small- x evolution kernel [33,22] for the WW-gluon distribution. We would like to emphasize that the final results with the Sudakov resummation will not depend on how we regulate the end-point singularity as shown in Refs. [23–25].

We can also calculate the virtual graphs, which have been shown in Fig. 4, where Fig. 4(a) contributes to both end-point singularity and small- x divergence and Fig. 4(b) only contributes to the small- x divergence. In particular, the contribution from Fig. 4(a) can be written as

$$\frac{\alpha_s}{2\pi} C_A \mathcal{F}^{(WW)}(x, k_{\perp}) \int_0^1 \frac{d\xi}{\xi(1-\xi)} \frac{d^2q_{\perp}}{(2\pi)^2} \frac{1}{q_{\perp}^2}, \quad (56)$$

where we can clearly separate out the above two contributions. For the end-point singularity term, we subtract it and put it in the soft factor from the Collins 2011 scheme, and obtain the same result as that in the collinear framework. Combining with the real gluon radiation contribution, we find that the finite end-point contribution leads to the Sudakov double logarithms.

It is a little bit more involved in the calculation of Fig. 4(b), for which we obtain,

$$\frac{\alpha_s}{2\pi} C_A \int_0^{\infty} \frac{d\xi}{\xi} \frac{d^2q_{\perp}}{(2\pi)^2} \frac{q_{\perp} \cdot (q_{\perp} - k_{g2\perp})(q_{\perp}^{\nu} - k_{g2\perp}^{\nu}) - q_{\perp}^{\nu} \epsilon_f^{\prime 2}/2}{q_{\perp}^2 ((q_{\perp} - k_{g2\perp})^2 + \epsilon_f^{\prime 2})} \Gamma_{AB}^{\nu} (k_{\perp}, k_{g2\perp}), \quad (57)$$

where $\epsilon_f^{\prime 2} = q_{\perp}^2/\xi$ and Γ'_{AB} is defined as

$$\Gamma'_{AB} = \int d^2x_1 d^2x_2 d^2x'_1 e^{ik_{g\perp} \cdot (x_{2\perp} - x'_{1\perp}) + ik_{g1\perp} \cdot (x_{1\perp} - x_{2\perp})} \times \frac{1}{2} \left(\text{Tr}[U^{\dagger}(x_2)U(x_{1\perp})] \text{Tr}[U^{\dagger}(x_{1\perp})U(x_2)] i\partial_{\perp}^{\nu} U^{\dagger}(x'_{\perp})U(x'_{\perp}) + h.c. \right). \quad (58)$$

It is important to notice that there is only small- x divergence when $\epsilon'_f = 0$. At this point, it is worthwhile to mention that the above results have been obtained by computing the virtual diagrams in the light cone gauge ($A^- = 0$) with the principal value prescription. One can also redo the calculation with other prescription and reproduce the same Collins–Soper and the BK evolution kernels.

Combining the real and virtual contributions, we can write down in the Fourier transformation conjugate variable r_\perp as in Sec. 2,

$$xG_{(-\infty)}^{(WW)}(x, r_\perp)|^{(1)} = \frac{\alpha_s}{2\pi} C_A \left\{ \left(\frac{-2}{\alpha_s} \right) \mathcal{F}^{(WW)}(r_\perp) \left[\frac{1}{2} \left(\ln \frac{\xi_c^2}{\mu^2} \right)^2 - \frac{1}{2} \left(\ln \frac{\xi_c^2 r_\perp^2}{c_0^2} \right)^2 \right] + \ln \left(\frac{1}{x} \right) \left(\frac{-2}{\alpha_s} \right) \int \mathbf{K}_{\text{DMMX}} \otimes \mathcal{F}^{(WW)}(x_g, r_\perp) \right\}, \quad (59)$$

where the finite terms combine the real gluon radiation and virtual contributions. With the above one-loop result, we can derive the Collins–Soper evolution equation for the TMD gluon. By solving the associated equations, we will be able to resum the Sudakov logarithms. Similarly, we can derive the small- x evolution, which resums the small- x logarithms.

With all order resummation we obtain the final results for the TMD gluon distribution as mentioned in the Introduction with Eq. (6).

$$xG_{(-\infty)}^{(WW)}(x, r_\perp, \xi_c^2 = Q^2) = -\frac{2}{\alpha_s} \int \frac{d^2x_\perp d^2y_\perp}{(2\pi)^4} e^{ik_\perp \cdot r_\perp} \mathcal{H}^{WW}(\alpha_s(Q)) e^{-S_{\text{pert}}^g(Q^2, r_\perp^2)} \times \mathcal{F}_{Y=\ln 1/x}^{WW}(x_\perp, y_\perp), \quad (60)$$

where $\mathcal{F}_{Y=\ln(1/x)}^{WW}$ is renormalized quadrupole gluon distributions defined in Eq. (7), and the Sudakov factor takes the same form as Eq. (33) in the last section, except now $B_g^{(1)} = 0$. The hard coefficient vanishes at one-loop order too: $\mathcal{H}^{WW} = 1 + \mathcal{O}(\alpha_s^2)$.

The result of $B_g^{(1)} = 0$ reflects the fact that the running of α_s is treated differently in the small- x CGC formalism than that in the collinear factorization formalism, where $B_g^{(1)}$ is proportional to β_0 . In particular, α_s running is part of the next-to-leading order BK evolution. However, in the collinear factorization, α_s running effects enters at the one-loop order (leading order in the DGLAP evolution). It is also related to the anomalous dimension for the integrated gluon distribution. Since we factorize the gluon TMD in terms of the integrated gluon distribution, we obtain $B_g^{(1)}$ as correspondent term from the anomalous dimension of the integrated gluon distribution. In the small- x calculations, however, the TMD gluon is calculated directly in the CGC formalism. There is no corresponding term related to the anomalous dimension with the integrated gluon distribution.

3.2.2. WW gluon distribution in DIS process

Now let us consider the WW gluon distribution in DIS type of processes [2,34], which only have final state interactions at LO. Because of the difference in the gauge link direction, there will be different diagrams contributing to the WW gluon distribution in the DIS process. We show the Feynman diagrams for this process in Fig. 5.

For this case, it is the diagrams in Fig. 5(a), (b) and (c) contribute to the terms depending on the adjoint representation Wilson line from $-\infty$ to $+\infty$, while the digram Fig. 5(d) contributes

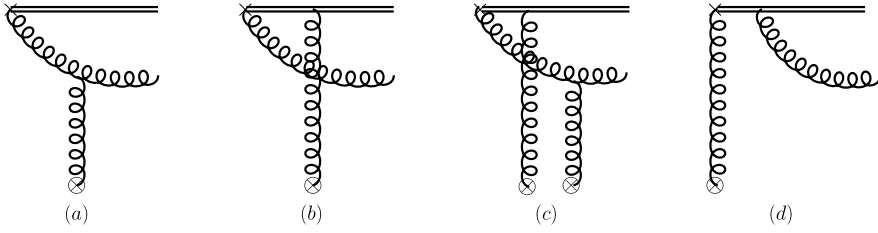


Fig. 5. The same as Fig. 3 but with the gauge link to $+\infty$. This gluon distribution can be used to describe the semi-inclusive process in eA collisions, such as the di-jet correlation in DIS process. Again, the crosses represent the probing gluon momentum (x, k_\perp) where x is the longitudinal momentum fraction and k_\perp is the transverse momentum.

to the end-point singularity. The calculations of these diagrams follow those for Fig. 3. The total contributions can be written as

$$\begin{aligned}
 \text{Fig. 5} &\propto \frac{k_{1\perp}^\alpha}{k_{1\perp}^2} \Gamma_A^{\nu'}(k_{g\perp}) \\
 &+ \int \frac{d^2 k_{g1\perp}}{(2\pi)^2} \left[\frac{k_{1\perp}^\alpha k_{1\perp}^{\nu'} - \epsilon_f^2 \frac{g_{1\perp}^{\alpha\nu'}}{2}}{k_{1\perp}^2 + \epsilon_f^2} - \frac{k_{\perp}^\alpha k_{\perp}^{\nu'} - \epsilon_f^2 \frac{g_{1\perp}^{\alpha\nu'}}{2}}{k_{\perp}^2 + \epsilon_f^2} \right] \Gamma_B'(k_{g1\perp}, k_{g2\perp}), \quad (61)
 \end{aligned}$$

where again $k_{1\perp} = k_\perp - k_{g\perp}$, $k'_{1\perp} = k_\perp - k_{g1\perp}$, $\epsilon_f^2 = \xi k_{1\perp}^2 / (1 - \xi)$ and $\Gamma_A^{\nu'}$ and Γ_B' are defined as

$$\begin{aligned}
 \Gamma_A^{\nu'} &= \int d^2 x_\perp e^{ik_{g\perp} \cdot x_\perp} \text{Tr} \left[T^b [i \partial_\perp^\nu U^\dagger(x_\perp) U(x_\perp), T^a] \right], \\
 \Gamma_B' &= \int d^2 x_{1\perp} d^2 x_{2\perp} e^{ik_{g1\perp} \cdot x_{1\perp} + ik_{g2\perp} \cdot x_{2\perp}} \frac{1}{T_F} \text{Tr} \left[U^\dagger(x_2) T^b U(x_2) U^\dagger(x_{1\perp}) T^a U(x_{1\perp}) \right]. \quad (62)
 \end{aligned}$$

The phase space integral for the real gluon radiations can be performed following the previous case, and we obtain the following result,

$$\begin{aligned}
 xG_{(+\infty)}^{(WW)}|_{real} &= \frac{\alpha_s}{2\pi^2} C_A \left\{ \int d^2 k_{g\perp} \left(\frac{-2}{\alpha_s} \right) \mathcal{F}^{(WW)}(x, k_{g\perp}) \frac{1}{(k_\perp - k_{g\perp})^2} \ln \frac{\zeta_c^2}{(k_\perp - k_{g\perp})^2} \right. \\
 &\quad \left. + \ln \left(\frac{1}{x} \right) \left(\frac{-2}{\alpha_s} \right) \int \mathbf{K}_{\text{DMMX}(r)} \otimes \mathcal{F}^{(WW)}(x_g, k_\perp) \right\}. \quad (63)
 \end{aligned}$$

Clearly, the Sudakov term and the small- x divergent term are the same as that in previous case. As mentioned in the previous subsection, we will have the same virtual contribution to the DIS-type gluon TMD. By adding the real and virtual contributions together, we can obtain the similar expression for the total result at one-loop order with the same Collins–Soper evolution and small- x evolution terms. Therefore, the resummation for the DIS-type gluon distribution is the same as that for the Drell–Yan type of gluon TMDs. Moreover, if one does not impose any lower cut off for ξ integration, one can show that the Drell–Yan like gluon TMD and the DIS gluon TMD are identical up to finite terms by playing the same mathematical trick applied to the quark TMD case. This demonstrates that our small x calculation is consistent with the universality argument. Therefore, after resummation, we have the same WW gluon distribution for the DIS-type and DY-type of processes.

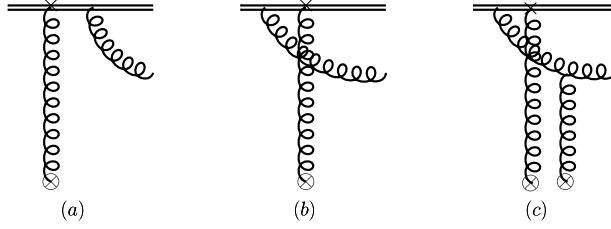


Fig. 6. Part of one-loop real gluon radiation diagrams for the dipole gluon distributions contributing to the Sudakov logarithms. This gluon distribution can be used to describe the photon–jet correlation in pA collisions. Again, the crosses represent the probing gluon momentum (x, k_\perp) where x is the longitudinal momentum fraction and k_\perp is the transverse momentum.

3.2.3. Dipole gluon distribution

Now, we turn to the dipole gluon distribution. The gauge link structure is very different from the previous cases. The leading order result can be expressed as

$$\begin{aligned}
 xG^{(dp)}(x, k_\perp) &= \frac{-2}{\alpha_s} \mathcal{F}^{(DP)}(x, k_\perp) \\
 &= -\frac{2}{\alpha_s} \int \frac{d^2x_\perp d^2y_\perp}{(2\pi)^4} e^{ik_\perp \cdot (x_\perp - y_\perp)} \nabla_{r_\perp}^{-2} \mathcal{F}^{(DP)}(x_\perp, y_\perp),
 \end{aligned} \tag{64}$$

where the dipole amplitude $\mathcal{F}^{(DP)}$ has been defined in the Introduction. In Figs. 6 and 7, we show the real gluon radiation at one-loop order.

The diagrams in Fig. 6 contribute to the Sudakov logarithms, and we get the following expression,

$$\begin{aligned}
 \text{Fig. 6} &\propto \int \frac{d^2x_\perp}{(2\pi)^2} e^{ik_{g\perp} \cdot x_\perp} \frac{k_{1\perp}^\alpha}{k_{1\perp}^2} [T^a \partial_\perp^\nu U(x_\perp)] - \int \frac{d^2k_{g1\perp} d^2x_1 d^2x_2}{(2\pi)^4} e^{ik_{g1\perp} \cdot (x_1 - x_2)} e^{ik_{g\perp} \cdot x_2} \\
 &\quad \times \frac{k_{1\perp}^\alpha - k_{g1\perp}^\alpha}{(k_\perp - k_{g1\perp})^2} [\partial_\perp^\nu U(x_1) U^\dagger(x_2) T^a U(x_2)].
 \end{aligned} \tag{65}$$

The amplitude squared of the above contribution can be calculated accordingly,

$$\begin{aligned}
 [\text{Fig. 6}]^2 &\propto 2 \int \frac{d\xi}{\xi(1-\xi)} \left\{ \frac{d^2x_\perp}{(2\pi)^2} e^{ik_{g\perp} \cdot (x_\perp - y_\perp)} \frac{1}{k_{1\perp}^2} C_F [\partial_\perp^\mu U(x_\perp) \partial_\perp^\mu U^\dagger(y_\perp)] \right. \\
 &\quad - \int \frac{d^2k_{g1\perp} d^2x_\perp d^2y_{1\perp} d^2y_{2\perp}}{(2\pi)^4} e^{ik_{g\perp} \cdot (x_\perp - y_{2\perp})} e^{-ik_{g1\perp} \cdot (y_{1\perp} - y_{2\perp})} \\
 &\quad \left. \times \frac{k_{1\perp} \cdot k'_{1\perp}}{k_{1\perp}^2 k'_{1\perp}{}^2} [T^a \partial_\perp^\mu U(x_\perp) U^\dagger(y_{2\perp}) T^a U(y_{2\perp}) \partial_\perp^\mu U^\dagger(y_{1\perp})] \right\}
 \end{aligned} \tag{66}$$

with $k'_{1\perp} = k_\perp - k_{g1\perp}$. By employing the identity,

$$\begin{aligned}
 &\text{Tr}[T^a \partial_\perp^\mu U(x_\perp) U^\dagger(y_{2\perp}) T^a U(y_{2\perp}) \partial_\perp^\mu U^\dagger(y_{1\perp})] \\
 &= \frac{1}{2} \text{Tr}[\partial_\perp^\mu U(x_\perp) U^\dagger(y_{2\perp})] \text{Tr}[U(y_{2\perp}) \partial_\perp^\mu U^\dagger(y_{1\perp})] - \frac{1}{2N_c} \text{Tr}[\partial_\perp^\mu U(x_\perp) \partial_\perp^\mu U^\dagger(y_{1\perp})],
 \end{aligned} \tag{67}$$

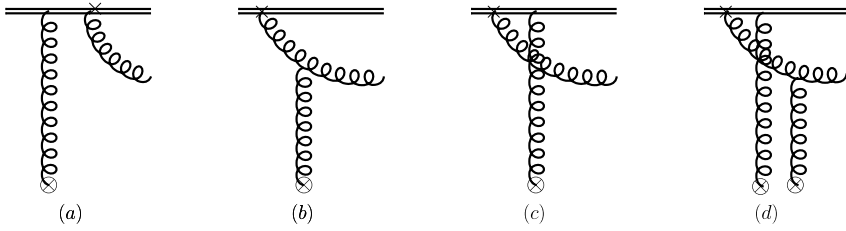


Fig. 7. Same as Fig. 6 but for part of BK-evolution contributions. Again, the crosses represent the probing gluon momentum (x, k_{\perp}) where x is the longitudinal momentum fraction and k_{\perp} is the transverse momentum.

one obtains,

$$\begin{aligned}
 [\text{Fig. 6}]^2 \propto & \int \frac{d\xi}{\xi(1-\xi)} \left\{ \frac{d^2x_{\perp}}{(2\pi)^2} e^{ik_{g\perp} \cdot (x_{\perp} - y_{\perp})} \frac{1}{k_{1\perp}^2} 2C_A \text{Tr}[\partial_{\perp}^{\mu} U(x_{\perp}) \partial_{\perp}^{\mu} U^{\dagger}(y_{\perp})] \right. \\
 & - \int \frac{d\xi}{\xi(1-\xi)} \int \frac{d^2k_{g1\perp} d^2x_{\perp} d^2y_{1\perp} d^2y_{2\perp}}{(2\pi)^4} e^{ik_{g\perp} \cdot (x_{\perp} - y_{2\perp})} e^{-ik_{g1\perp} \cdot (y_{1\perp} - y_{2\perp})} \\
 & \left. \times \frac{k_{1\perp} \cdot k'_{1\perp}}{k_{1\perp}^2 k'_{1\perp}{}^2} \text{Tr}[\partial_{\perp}^{\mu} U(x_{\perp}) U^{\dagger}(y_{2\perp})] \text{Tr}[U(y_{2\perp}) \partial_{\perp}^{\mu} U^{\dagger}(y_{1\perp})] \right\}. \tag{68}
 \end{aligned}$$

After the end point singularity in the first term is regularized by subtracting the soft factor in the Collins-11 scheme, the desired Sudakov logarithm can be recovered. The second term is a bit troublesome as the end point singularity is associated with three point function. To get rid of this contribution, our argument goes as follows. First of all an additional hard scale is always required for justifying the use of TMD factorization. In the current case, the radiated gluon transverse momentum plays the role of the hard scale, which implies $k_{\perp} \gg k_{g\perp} \sim k_{g1\perp}$. When we ignore $k_{g\perp}$ and $k_{g1\perp}$ in the second term, we can carry out some integrations trivially and reduce the three point function to the two point function $\text{Tr}[\partial_{\perp}^{\mu} U(x_{\perp}) U^{\dagger}(y_{2\perp})] \text{Tr}[U(y_{2\perp}) \partial_{\perp}^{\mu} U^{\dagger}(y_{2\perp})]$ which apparently vanishes.

Besides, the above term also contributes to the small- x divergence. Additional diagrams are shown in Fig. 7, which can be written as

$$\begin{aligned}
 \text{Fig. 7} \propto & \int \frac{d^2x_{1\perp} d^2x_{2\perp} d^2k_{g1\perp}}{(2\pi)^4} e^{ik_{g1\perp} \cdot (x_{1\perp} - x_{2\perp})} e^{ik_{g\perp} \cdot x_{2\perp}} \left[U(x_1) U^{\dagger}(x_2) T^a U(x_2) \right] \\
 & \times \frac{1}{2} \left[\frac{k_{1\perp}^{\alpha} k_{1\perp}^{\nu} - \epsilon_f^2 \frac{g_{\perp}^{\alpha\nu}}{2}}{k_{1\perp}^2 + \epsilon_f^2} - \frac{k_{1\perp}^{\alpha} k_{1\perp}^{\nu} - \epsilon_f^2 \frac{g_{\perp}^{\alpha\nu}}{2}}{k_{1\perp}^2 + \epsilon_f^2} \right], \tag{69}
 \end{aligned}$$

where again $k_{1\perp} = k_{\perp} - k_{g\perp}$, $k'_{1\perp} = k_{\perp} - k_{g1\perp}$, $\epsilon_f^2 = \xi k_{1\perp}^2 / (1 - \xi)$. To check the BK-evolution, we perform the partial integral of Eq. (65), and take $\xi = 0$ of Eq. (69), and add them together,

$$\begin{aligned}
 \text{Figs. 6, 7}|_{BK} \propto & k_{\perp}^{\nu} \int \frac{d^2x_{\perp}}{(2\pi)^2} e^{ik_{g\perp} \cdot x_{\perp}} \frac{k_{1\perp}^{\alpha}}{k_{1\perp}^2} [T^a U(x_{\perp})] \\
 & - k_{\perp}^{\nu} \int \frac{d^2k_{g1\perp} d^2x_1 d^2x_2}{(2\pi)^4} e^{ik_{g1\perp} \cdot (x_1 - x_2)} e^{ik_{g\perp} \cdot x_2} \frac{(k_{\perp} - k_{g1\perp})^{\alpha}}{(k_{\perp} - k_{g1\perp})^2} \\
 & \times [U(x_1) U^{\dagger}(x_2) T^a U(x_2)], \tag{70}
 \end{aligned}$$

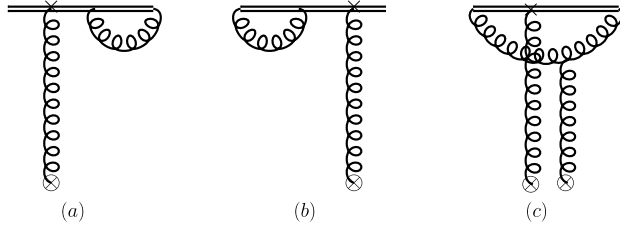


Fig. 8. Virtual gluon radiation diagrams for the dipole gluon distribution at one-loop order. These diagrams contribute to the Sudakov and small- x logarithms. Again, the crosses represent the probing gluon momentum (x, k_\perp) where x is the longitudinal momentum fraction and k_\perp is the transverse momentum.

where the bracket in the above equation is exactly the real gluon contribution to the BK-evolution for the dipole scattering amplitude.

We can also carry out the phase space integral, and arrive at the following result for the real gluon radiation contribution to the dipole-gluon distribution at one-loop order,

$$xG^{(DP)}_{real}^{(1)} = \frac{\alpha_s}{2\pi^2} C_A \left\{ \int d^2k_{g\perp} \left(-\frac{2}{\alpha_s}\right) \mathcal{F}^{(DP)}(x, k_{g\perp}) \frac{k_{g\perp}^2}{(k_\perp - k_{g\perp})^2} \ln \frac{\zeta_c^2}{(k_\perp - k_{g\perp})^2} + \ln\left(\frac{1}{x}\right) \left(-\frac{2}{\alpha_s}\right) k_\perp^2 \int \mathbf{BK}_{(r)} \otimes \mathcal{F}^{(DP)}(x, k_{g\perp}) \right\}. \quad (71)$$

Similarly, we can calculate the virtual diagrams, which are shown in Figs. 8, 9. The calculation of diagrams of Fig. 8(a, b) is the same as that in Fig. 4(a). Their contributions, together with the sub-leading N_c contribution from Fig. 8(c), lead to the following expression,

$$\frac{\alpha_s}{2\pi} C_A \int_0^1 \frac{dz}{z(1-z)} \frac{d^2q_\perp}{(2\pi)^2} \frac{1}{q_\perp^2}. \quad (72)$$

The leading N_c contribution from Fig. 8(c) leads to

$$\frac{\alpha_s}{2\pi} C_A \int \frac{dz}{z(1-z)} \frac{q_\perp \cdot (q_\perp - k_{g2\perp})}{q_\perp^2 (q_\perp - k_{g2\perp})^2} k_{g1\perp}^v k_\perp^v \Gamma_{AB}^{(dp)}, \quad (73)$$

where $\Gamma_{AB}^{(dp)}$ is defined as

$$\Gamma_{AB}^{(dp)} = \int_0^1 d^2x_1 d^2x_2 d^2x'_\perp e^{ik_\perp \cdot (x_{2\perp} - x'_\perp) + ik_{g1\perp} \cdot (x_{1\perp} - x_{2\perp})} \times \text{Tr}[U(x_2)U^\dagger(x'_\perp)] \text{Tr}[U(x_1)U^\dagger(x_2)]. \quad (74)$$

It is interesting to find out that the diagrams of Fig. 9(a, b) vanish, and the calculations of Fig. 9(c, d) are similar to those in Fig. 4(c). We will have the following expression,

$$\frac{\alpha_s}{2\pi} C_A \int_0^\infty \frac{d\xi}{\xi} \frac{d^2q_\perp}{(2\pi)^2} \frac{q_\perp \cdot (q_\perp - k_{g2\perp})(q_\perp^v - k_{g2\perp}^v) - q_\perp^v \epsilon_f^2/2}{q_\perp^2 ((q_\perp - k_{g2\perp})^2 + \epsilon_f^2)} k_\perp^v \Gamma_{AB}^{(dp)}(k_\perp, k_{g2\perp}), \quad (75)$$

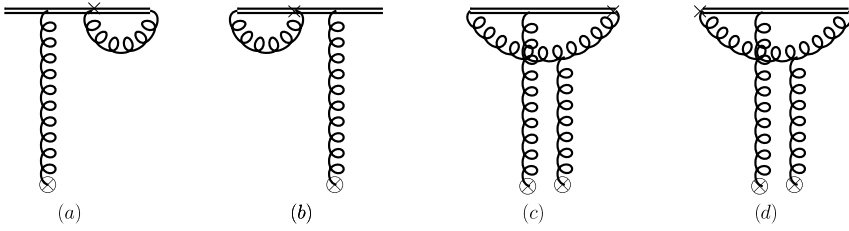


Fig. 9. Same as Fig. 8 but for part of BK-evolution contributions. Again, the crosses represent the probing gluon momentum (x, k_\perp) where x is the longitudinal momentum fraction and k_\perp is the transverse momentum.

where $\epsilon_f^2 = q_\perp^2/\xi$ and $\Gamma_{AB}^{(dp)}$ is defined as Eq. (74). The above equation only contributes to the small- x divergence. The total contributions for the small- x divergence from the above equations can be summarized as,

$$k_\perp^\nu k_\perp^\nu \frac{\alpha_s}{2\pi} \int \frac{dz}{1-z} \frac{d^2 q_\perp}{(2\pi)^2} \left[\frac{1}{q_\perp^2} - \frac{q_\perp \cdot (q_\perp - k_{g2\perp})}{q_\perp^2 (q_\perp - k_{g2\perp})^2} \right] \Gamma_{AB}^{(dp)}(k_\perp, k_{g2\perp}), \tag{76}$$

which is the virtual contribution to the BK evolution of the dipole amplitude.

Adding the real and virtual contributions together, we have the total contribution at one-loop order,

$$\begin{aligned} &xG^{(DP)}(x, r_\perp)|^{(1)} \\ &= \frac{\alpha_s}{2\pi} C_A \left\{ \left(-\frac{2}{\alpha_s}\right) \nabla_{r_\perp}^{-2} \mathcal{F}^{(DP)}(x, r_\perp) \left[\frac{1}{2} \left(\ln \frac{\zeta_c^2}{\mu^2}\right)^2 - \frac{1}{2} \left(\ln \frac{\zeta_c^2 r_\perp^2}{c_0^2}\right)^2 \right] \right. \\ &\quad \left. + \ln\left(\frac{1}{x}\right) \left(-\frac{2}{\alpha_s}\right) \nabla_{r_\perp}^{-2} \int \mathbf{K}_{BK} \otimes \mathcal{F}^{(DP)}(x, r_\perp) \right\}. \end{aligned} \tag{77}$$

The above result is almost the same as that in previous subsection for the WW -gluon distribution. Again, we have double logarithms associated with Sudakov effects and the small- x logarithms, and the associated evolution equations can be derived as well. After resummation, we obtain the all order result as

$$\begin{aligned} xG^{(DP)}(x, r_\perp, \zeta_c = Q) &= -\frac{2}{\alpha_s} \int \frac{d^2 x_\perp d^2 y_\perp}{(2\pi)^4} e^{ik_\perp \cdot r_\perp} \mathcal{H}^{DP}(\alpha_s(Q)) e^{-S_{peri}^s(Q^2, r_\perp^2)} \\ &\quad \times \nabla_{r_\perp}^{-2} \mathcal{F}_{Y=\ln 1/x}^{DP}(x_\perp, y_\perp), \end{aligned} \tag{78}$$

where $\mathcal{F}_{Y=\ln 1/x}^{DP}$ is renormalized dipole gluon distribution of Eq. (10) and $\mathcal{H}^{DP} = 1 + \mathcal{O}(\alpha_s^2)$. The Sudakov factor follows the same as that for WW -gluon distribution in the last subsection, where again $B_g^{(1)} = 0$ by the same reason.

4. Conclusion

In summary, we have shown that one can treat both the Collins–Soper evolution and the BK evolution of small x parton TMDs simultaneously in a unified and consistent framework. To achieve so, we compute small x gluon TMDs in the Collins-11 scheme using the CGC approach. The resulting hard parts contain two different type large logarithms which can be resummed by

means of the Collins–Soper equation and the BK equation, respectively. We emphasize that the relative size of two type large logarithms is solely determined by the kinematics of a physical process which involve three well separated scales. The evolved small x gluon TMD eventually can be expressed as the convolution of the Sudakov form factor and the renormalized dipole amplitudes. In other words, at small x , gluon TMDs can be matched onto dipole scattering amplitudes rather than the normal PDFs in the collinear approach.

Our analysis is applied to the quark distribution, as well as the WW gluon TMD and the dipole gluon TMD cases. For the quark distribution and the WW gluon cases, we compute the parton TMDs involving a past pointing gauge link as well as these involving a future pointing gauge link. Though it appears to be rather nontrivial, the DIS type and the Drell–Yan type parton TMDs are shown to be identical as expected from the universality argument. As a final remark, we also point out that in order to recover the correct Sudakov factor, it is critical to calculate gluon TMDs using their matrix elements definition given in Eqs. (1), (4) instead of these in Eqs. (3), (5), since the gluon distributions defined in latter equations have already put gauge links on the light-cone.

Finally, we consider the present work as one more attempt to advance the study of the topical issue: the interplay of small x physics and TMD/spin physics. It shall provide a theoretical ground for performing phenomenological analysis of the relevant physical observables that can be measured at RHIC, LHC and the planned EIC.

Acknowledgements

This material is based upon work supported by the U.S. Department of Energy, Office of Science, Office of Nuclear Physics, under contract number DE-AC02-05CH11231, and within the framework of the TMD Topical Collaboration. This work is also supported by the National Science Foundation of China under Grant Nos. 11675093, 11575070, and by the Thousand Talents Plan for Young Scientist.

References

- [1] L.D. McLerran, R. Venugopalan, *Phys. Rev. D* 49 (1994) 2233;
L.D. McLerran, R. Venugopalan, *Phys. Rev. D* 49 (1994) 3352;
L.D. McLerran, R. Venugopalan, *Phys. Rev. D* 50 (1994) 2225.
- [2] Y.V. Kovchegov, A.H. Mueller, *Nucl. Phys. B* 529 (1998) 451, arXiv:hep-ph/9802440.
- [3] J.C. Collins, D.E. Soper, *Nucl. Phys. B* 194 (1982) 445.
- [4] X.d. Ji, J.P. Ma, F. Yuan, *J. High Energy Phys.* 0507 (2005) 020, arXiv:hep-ph/0503015.
- [5] D. Kharzeev, Y.V. Kovchegov, K. Tuchin, *Phys. Rev. D* 68 (2003) 094013, arXiv:hep-ph/0307037.
- [6] C.J. Bomhof, P.J. Mulders, F. Pijlman, *Eur. Phys. J. C* 47 (2006) 147, arXiv:hep-ph/0601171.
- [7] F. Dominguez, B.W. Xiao, F. Yuan, *Phys. Rev. Lett.* 106 (2011) 022301, arXiv:1009.2141 [hep-ph].
- [8] F. Dominguez, C. Marquet, B.W. Xiao, F. Yuan, *Phys. Rev. D* 83 (2011) 105005, arXiv:1101.0715 [hep-ph].
- [9] C. Marquet, E. Petreska, C. Roiesnel, *J. High Energy Phys.* 1610 (2016) 065, arXiv:1608.02577 [hep-ph].
- [10] A. Metz, J. Zhou, *Phys. Rev. D* 84 (2011) 051503, arXiv:1105.1991 [hep-ph].
- [11] F. Dominguez, J.W. Qiu, B.W. Xiao, F. Yuan, *Phys. Rev. D* 85 (2012) 045003, arXiv:1109.6293 [hep-ph].
- [12] J. Zhou, *Phys. Rev. D* 89 (7) (2014) 074050, arXiv:1308.5912 [hep-ph].
- [13] D. Boer, M.G. Echevarria, P. Mulders, J. Zhou, *Phys. Rev. Lett.* 116 (12) (2016) 122001, arXiv:1511.03485 [hep-ph].
- [14] D. Boer, S. Cotogno, T. van Daal, P.J. Mulders, A. Signori, Y.J. Zhou, *J. High Energy Phys.* 1610 (2016) 013, arXiv:1607.01654 [hep-ph].
- [15] I. Balitsky, *Nucl. Phys. B* 463 (1996) 99.
- [16] Y.V. Kovchegov, *Phys. Rev. D* 60 (1999) 034008.

- [17] J.C. Collins, D.E. Soper, Nucl. Phys. B 193 (1981) 381;
J.C. Collins, D.E. Soper, Nucl. Phys. B 213 (1983) 545 (Erratum).
- [18] J. Zhou, J. High Energy Phys. 1606 (2016) 151, arXiv:1603.07426 [hep-ph].
- [19] I. Balitsky, A. Tarasov, J. High Energy Phys. 1510 (2015) 017, arXiv:1505.02151 [hep-ph];
I. Balitsky, A. Tarasov, J. High Energy Phys. 1606 (2016) 164, arXiv:1603.06548 [hep-ph].
- [20] S. Marzani, Phys. Rev. D 93 (5) (2016) 054047, arXiv:1511.06039 [hep-ph].
- [21] A.H. Mueller, B.W. Xiao, F. Yuan, Phys. Rev. Lett. 110 (8) (2013) 082301, arXiv:1210.5792 [hep-ph].
- [22] A.H. Mueller, B.W. Xiao, F. Yuan, Phys. Rev. D 88 (11) (2013) 114010, arXiv:1308.2993 [hep-ph].
- [23] S. Catani, D. de Florian, M. Grazzini, Nucl. Phys. B 596 (2001) 299, arXiv:hep-ph/0008184.
- [24] S. Catani, L. Cieri, D. de Florian, G. Ferrera, M. Grazzini, Nucl. Phys. B 881 (2014) 414, arXiv:1311.1654 [hep-ph].
- [25] A. Prokudin, P. Sun, F. Yuan, Phys. Lett. B 750 (2015) 533, arXiv:1505.05588 [hep-ph].
- [26] J.C. Collins, Foundations of Perturbative QCD, Cambridge University Press, Cambridge, 2011.
- [27] J. Jalilian-Marian, A. Kovner, A. Leonidov, H. Weigert, Nucl. Phys. B 504 (1997) 415;
J. Jalilian-Marian, A. Kovner, A. Leonidov, H. Weigert, Phys. Rev. D 59 (1999) 014014;
E. Iancu, A. Leonidov, L.D. McLerran, Nucl. Phys. A 692 (2001) 583.
- [28] See a review, E. Iancu, R. Venugopalan, arXiv:hep-ph/0303204.
- [29] J.C. Collins, D.E. Soper, G. Sterman, Nucl. Phys. B 250 (1985) 199.
- [30] L.D. McLerran, R. Venugopalan, Phys. Rev. D 59 (1999) 094002;
R. Venugopalan, Acta Phys. Pol. B 30 (1999) 3731.
- [31] A.H. Mueller, Nucl. Phys. B 558 (1999) 285.
- [32] C. Marquet, B.W. Xiao, F. Yuan, Phys. Lett. B 682 (2009) 207, arXiv:0906.1454 [hep-ph].
- [33] F. Dominguez, A.H. Mueller, S. Munier, B.W. Xiao, Phys. Lett. B 705 (2011) 106, arXiv:1108.1752 [hep-ph].
- [34] Y.p. Xie, X. Chen, Phys. Rev. D 89 (7) (2014) 074040, arXiv:1312.7543 [hep-ph].